Pharmaceutical Research, Volume 23, No. 2, February 2006 (© 2006)
DOI: 10.1007/s11095-005-9305-2

Research Paper

Pharmacologic and Pharmacokinetic Assessment of Anti-TGFβ2 Aptamers in Rabbit Plasma and Aqueous Humor

Thomas G. McCauley,[1,2] Jeffrey C. Kurz,[1] Patricia G. Merlino,[1] Scott D. Lewis,[1] Madaline Gilbert,[1] David M. Epstein,[1] and H. Nicholas Marsh[1]

Received May 17, 2005; accepted October 31, 2005

Purpose. The aim of the study is to determine the bioactivity and effects of PEGylation on the pharmacokinetics in rabbit aqueous humor and plasma of an aptamer directed against TGFβ2.
Methods. Pharmacological activity of anti-TGFβ2 aptamer in rabbit ocular fluid was demonstrated using a mink lung epithelial cell proliferation assay. For pharmacokinetic analyses, concentrations of aptamers in plasma and aqueous humor were determined over time following bilateral subconjunctival administration to Dutch-belted rabbits using a hybridization-based pseudo-enzyme-linked immunosorbent assay (ELISA) assay.
Results. Anti-TGFβ2 aptamer (ARC81) binds to human TGFβ2 with a K_D of approximately 5 nM and inhibits the activity of human TGFβ2 *in vitro* in a cell-based assay with an IC_{50} of approximately 100 nM. ARC81 blocks endogenously derived TGFβ2 in rabbit aqueous humor *in vitro* with an IC_{50} of approximately 200 nM and an IC_{90} of approximately 1 μM. *In vivo* in rabbit, ARC81 [no polyethylene glycol (PEG)] entered systemic circulation rapidly (t_{max} = 1 h in plasma) relative to aptamer conjugates ARC117 (20 kDa PEG) and ARC119 (40 kDa PEG), which showed prolonged residence in the subconjunctival space and aqueous compartment (t_{max} = 6 and 12 h, respectively, in plasma). Both 20- and 40-kDa aptamer conjugates reached maximal concentrations (C_{max}) in aqueous humor of 23–30 nM and remained at or above 1 nM for as long as 12 h.
Conclusions. Pharmacologically active levels of anti-TGFβ2 aptamers can be sustained in the ocular fluid and local tissue environment over a 12-h period after single administration. Daily subconjunctival administration of PEGylated anti-TGFβ2 aptamers should allow further pharmacological evaluation of these agents in a rabbit conjunctival scarring model. Perioperative administration, via subconjunctival injection, may prove to be an effective means to deliver therapeutic quantities of TGFβ2 aptamer conjugates in trabeculectomy procedures.

KEY WORDS: aptamer; glaucoma; ocular pharmacokinetics; TGFβ2 inhibitor; PEGylation.

INTRODUCTION

Glaucoma is a proliferative disease of the eye and a leading cause of vision loss leading to blindness. The disease is associated with reduced fluid drainage from the eye and an elevation in intraocular pressure (IOP). When IOP is high, individual nerve fiber cells die, restricting vision. Glaucoma progression is currently irreversible, but it may be slowed with therapeutic drugs to modulate fluid production and IOP. The first line of glaucoma treatment is typically the use of therapeutic drugs to modulate intraocular fluid levels. Glaucoma filtering microsurgery, or trabeculectomy, is a second line of treatment in which a tiny puncture is made in the sclera of the eye to allow fluid to drain into a bleb, thereby reducing IOP. However, postsurgical complications are significant and can lead to continued vision loss. Complications from surgery arise when incomplete wound healing and scarring results in a return to high IOP and a need for additional surgery. Antimetabolite agents, such as mitomycin-C and 5-fluorouracil, are currently used to control the extent of postsurgical scarring (1). However, severe complications can arise from repeat trabeculectomies and the use of antimetabolite therapy. These include fluid leakage, intraocular hypotony (low IOP), and general tissue toxicity (2–4). Antimetabolite agents can further damage eye tissue leading to low IOP or even blindness. Failure of antimetabolite therapy in glaucoma treatment is defined by a two-line drop in Snellen visual acuity tests (5).

Progression of glaucoma disease is associated with increases in levels of transforming growth factor cytokines in the eye (6). The transforming growth factor β (TGFβ subfamily) is comprised of three members: TGFβ1, TGFβ2, and

[1] Aptamer Pharmacology Group, Archemix Corp., 1 Hampshire Street, Cambridge, Massachusetts 02139, USA.
[2] To whom correspondence should be addressed. (e-mail: mccauley@archemix.com)

ABBREVIATIONS: AUC, area under the concentration *vs.* time curve; C_{max}, highest concentration observed; MLEC, mink lung epithelial cell; NCA, noncompartmental analysis; PEG, polyethylene glycol; SELEX, systematic evolution of ligands by exponential enrichment; $t_{1/2}$, terminal half–life; t_{max}, time at which the highest concentration occurred; V_d, volume of distribution.

TFGβ3. Transforming growth factor beta 2 (TGFβ2) is a 25-kDa homodimer that is involved in cell proliferation, differentiation, and extracellular matrix formation. TGFβ2 is implicated in ocular wound healing and is suggested to play a role in scarring associated with glaucoma surgery (7). After trabeculectomy, aqueous humor bathes the surgical wound, and levels of TGFβ2 have been reported to be related to the aqueous concentration and the breakdown of the blood–aqueous barrier (19). Elevated levels of TGFβ2 are detected in aqueous humor in glaucomatous eyes compared to control levels in normal eyes: 21 pM glaucomatous *vs.* 12 pM for normal eyes (6). A rabbit model of conjunctival scarring has been used to assess the efficacy of the antimetabolites including mitomycin-C and 5-fluorouracil. Recently, TGFβ2 has been implicated as a causative agent in ocular scarring in both the rabbit conjunctival scarring model and in human disease, and as such, the rabbit model has also been used to evaluate antagonists of TGFβ2 (7–9).

The present study describes pharmacologic and pharmacokinetic characteristics of aptamer inhibitors of TGFβ2. Aptamers are rapidly becoming established as a new class of nucleic acid-based medicines. The mechanism by which aptamers inhibit the function of their targets is fundamentally different from that of other therapeutic nucleic acids such as antisense or siRNA. Rather than disrupting synthesis of a target protein by sequence-dependent hybridization with its mRNA, aptamers fold into distinctive three-dimensional structures that bind to and inhibit target proteins directly with high affinity and specificity. Thus, aptamers operate in a manner that is more similar mechanistically to monoclonal antibodies or to small molecule drugs than to other nucleic acid-based pharmaceuticals. Aptamer inhibitors of a wide array of protein targets have been generated using an iterative process of selection and amplification [systematic evolution of ligands by exponential enrichment (SELEX)] (10). Chemical modifications such as incorporation of 2′-fluoro or 2′-*O*-methyl nucleotides at the ribose 2′-hydroxyl position render aptamers highly resistant to nuclease degradation in plasma (11). Similarly, chemical conjugation (PEGylation) to high molecular weight polymers [e.g., polyethylene glycols (PEGs)] protects aptamers from renal filtration *in vivo* and promotes persistence of aptamers in circulation (12,13). These improvements in nuclease resistance and pharmacokinetic properties have enabled a variety of clinical applications of aptamers.

Here, we report the pharmacological evaluation of aptamer inhibitors and their potential to block both human and rabbit isoforms of TGFβ2. We also describe the function of anti-TGFβ2 aptamer in rabbit aqueous humor, an endogenous source of TGFβ2. Finally, we describe the pharmacokinetic characterization of anti-TGFβ2 aptamers upon injection into rabbit subconjuctiva as a prelude to further preclinical evaluation of such agents to reduce postsurgical scarring associated with glaucoma treatment.

MATERIALS AND METHODS

Aptamer Sequences

Nucleotide sequences of anti-TGFβ2 aptamers (14) are indicated below. Lowercase letters f and m denote stabilizing 2′-fluoro and 2′-*O*-methyl substitutions, respectively. At the 3′ terminus, 3T denotes an inverted dT cap structure. Presence of the 5′-amine (NH_2) facilitates chemical coupling to PEG species.

ARC81: 5′-NH_2-mGmGmGmGfUfUAfUfUmAfC-mAmGmAmGfUfCfUGfUAfUAmGfCfUmGfU-mAfCfCfC-3T-3′

ARC117: 5′-[20 kDa PEG]-NH_2-mGmGmGmGfU-fUAfUfUmAfCmAmGmAmGfUfCfUGfUAfUAmGfC-fUmGfUmAfCfCfC-3T-3′

ARC119: 5′-[40 kDa PEG]-NH_2-mGmGmGmGfU-fUAfUfUmAfCmAmGmAmGfUfCfUGfUAfUAmGfC-fUmGfUmAfCfCfC-3T-3′

ARC77: 5′-OH-GGAGGfUfUAfUfUAfCAGAG-fUfCfUGfUAfUAGfCfUGfUAfCfUfCfC-3T-3′

Oligonucleotide Synthesis

Synthesis of ARC81 was performed using standard solid-phase phosphoramidite chemistry, followed by ion-exchange high-pressure liquid chromatography (HPLC) or polyacrylamide gel electrophoresis (PAGE) purification. ARC77 was prepared by transcription using a Durascribe kit (Epicentre, Madison, WI, USA) followed by PAGE purification.

Synthesis of Aptamer Conjugates

ARC81 was conjugated to either 20 or 40 kDa polyethylene glycol to generate ARC117 (20 kDa PEG) and ARC119 (40 kDa PEG). For PEG conjugation, ARC81 was dissolved to 1 mM in 100 mM sodium carbonate buffer, pH 8.5, and was reacted for 1 h with a 2.5 M excess of mPEG–succinimidyl propionate (MW 20 kDa, Nektar Therapeutics, Huntsville, AL, USA) or mPEG2-NHS ester (MW 40 kDa) (Shearwater Corp., Huntsville, AL, USA) in an equal volume of acetonitrile. The resulting products were then purified by reverse-phase HPLC on a Transgenomic OligoPrep HC column with acetonitrile, 50 mM triethylammonium acetate as an eluent.

TGFβ2 Protein

Purified human TGFβ2 was obtained from R&D Systems (Minneapolis, MN, USA), and its biochemical activity was verified by activation of TGFβ2-dependent signaling using the mink lung epithelial cell (MLEC) proliferation assay described below.

Binding of TGFβ2 Protein to Anti-TGFβ2 Aptamers

The dissociation constant for the binding of ARC77 to purified human TGFβ2 protein was determined by nitrocellulose-filter partitioning using ^{32}P-labeled RNA. Binding reactions were initiated by the addition of aptamer (≤0.1 nM) in binding buffer (50 mM HEPES, pH 7.4, 1 mM $MgCl_2$, 1 mM $CaCl_2$, 3 mM KCl, 140 mM NaCl, 0.1 mg/ml BSA, 0.01 mg/ml tRNA) to excess TGFβ2 protein (0.2–100 nM). Following 10- to 30-min incubation at room temperature, protein-bound aptamer was separated from unbound aptamer by vacuum filtration using a Minifold® I, 96-well Dot-Blot manifold

(Schleicher & Schuell, Keene, NH, USA). Protein-bound aptamer and residual-free aptamer were captured, respectively, on prewetted Protran nitrocellulose (Schleicher & Schuell) and Hybond-P polyvinylidene difluoride (Amersham Biosciences, Piscataway, NJ, USA) and analyzed as described (15).

ARC81, which contains a number of 2′-methoxy functional groups as well as a 5′-amine, was less amenable to binding analysis by the method described above because of nonspecific interactions with the nitrocellulose membrane. Hence, the affinity of this aptamer was assessed by its ability to inhibit the interaction between TGFβ2 and ^{32}P-labeled ARC77. Competitive binding reactions were prepared by incubation in binding buffer of ^{32}P-labeled ARC77 (≤0.1 nM) with 2.5 nM TGFβ2 protein and increasing concentrations of unlabeled, competitor aptamer (0.05–300 nM). For each concentration of competitor, the amount of residual protein-bound ^{32}P-labeled ARC77 was quantified by nitro-cellulose filtration. The data were normalized to control samples lacking competitor and plotted as percent inhibition *vs.* competitor oligonucleotide concentration to obtain IC_{50} values. Dissociation constants were calculated from IC_{50} values according to the relationship $K_C = IC_{50}/(1 + [TGF\beta2]/K_D)$, where K_C is the dissociation constant for competitor and K_D is the dissociation constant for ^{32}P-labeled ARC77.

Activation of TGFβ2 in Aqueous Humor

Latent TGFβ2 was activated by transient acidification as described by Cousins *et al.* (18). Briefly, the pH of rabbit aqueous humor (Pel-Freez Biologicals, Rogers, AR, USA) was lowered to 3.0 with 100 mM HCl for 2 min. The aqueous humor was then brought to neutral pH (7.5–8.0) with 100 mM NaOH/phosphate-buffered saline (PBS) and tested at 1.58% vol/vol.

Mink Lung Epithelial Cell Proliferation Assay

Mink lung epithelial cells were plated at 4000 cells per well in black 96-well plates (Nunc, Rochester, NY, USA) in Dulbecco's modified Eagle's medium (Invitrogen, Chicago, IL, USA) containing 1% penicillin/streptomycin (Invitrogen) and 0.5% fetal bovine serum (Invitrogen). Cells were incubated at 37°C in 5% CO_2 for 4 h to allow adherence of cells. Aptamer, aqueous humor (Pel-Freez), anti-TGFβ2 antibody (R&D Systems), and/or TGFβ2 (R&D Systems) were simultaneously added to the cells at the indicated concentrations. Treated cells were incubated at 37°C in 5% CO_2 for 16 h. Cell proliferation was measured using a chemiluminescent BrdU kit as per manufacturer's instructions (Roche, Indianapolis, IN, USA). Plates were read by a TopCount microplate scintillation and luminescence counter (Packard Bioscience Co., Downers Grove, IL, USA).

Animals and Experimental Procedures

Aptamers were administered to Dutch-belted rabbits (Covance, Denver, PA, USA). At the onset of treatment, the animals were 6 months in age, and their body weights ranged from 1.7 to 2.5 kg. Rabbits were housed individually in stainless-steel cages equipped with a mesh-bottom floor and an automatic watering valve. Environmental conditions during the study conduct were controlled at a target temperature and relative humidity of 17 ± 3°C and 50 ± 20%, respectively. The photoperiod was 12-h light and 12-h dark except when interrupted because of scheduled activities. Animals were fed with a standard certified pelleted commercial laboratory diet (PMI Certified Rabbit 5322: PMI Nutrition International Inc., Richmond, IN, USA). All animals had free access to 180 g of food per day, except during protocol-designated procedures. Water was available to the animals *ad libitum* except during designated procedures. An acclimation period of approximately 1 week was allowed between animal receipt and treatment to accustom the animals to the laboratory environment. During the acclimation, all animals were weighed and assigned randomly to treatment groups as follows (see below):

Three spare animals were subsequently allocated to group 5, numbered 501–503, and administered formulation vehicle only to provide extra control aqueous fluid, vitreous fluid, and plasma for use in the hybridization assay.

Aptamer Formulations and Reagents

Test articles ARC81, ARC117, and ARC119 were formulated in PBS (Sigma-Aldrich, St. Louis, MO, USA) at a concentration of 10 mg/ml and filtered through a 0.22-μM Millex™ filter (Millipore, Billerica, MA, USA) into sterile vials. Vials were stored frozen at −20°C until use. The vehicle administered to control animals consisted of sterile-filtered (0.22 μM) phosphate-buffered saline. A 1:10,000 solution (equivalent to 0.1 mg/ml) of benzalkonium chloride 50% NF (Spectrum Lab Products, Inc., Gardena, CA, USA) was prepared by diluting with the appropriate volume of 0.9% sodium chloride (US Pharmacopoeia).

Aptamer Administration

All animals were anesthetized prior to aptamer administration. Immediately prior to anesthesia, mydriatic drops (1% Mydriacyl) were applied to the eyes. Topical antibiotic (gentamicin ophthalmic drops) was applied to each eye once on the day before treatment, once immediately following injection, and twice on the day following injection (AM and PM). Prior to dosing, the animals received an intramuscular sedative injection of a ketamine and xylazine cocktail, and the conjunctiva of each eye was flushed with benzalkonium

Group no.	Test article	Dose level	PEG group	Dose level	Dose volume	Animals/time point
1	None (vehicle)	NA	None	NA	0.1 ml/eye	3
2	ARC81	1 mg/eye	None	1 mg/eye	0.1 ml/eye	3
3	ARC117	1 mg/eye	20 kDa	1 mg/eye	0.1 ml/eye	3
4	ARC119	1 mg/eye	40 kDa	1 mg/eye	0.1 ml/eye	3

chloride diluted in 0.9% sodium chloride USP to 1:10,000 (v/v). A local anesthetic (Alcain, 0.5%) was applied to each eye. Subconjuctival injection of aptamers was performed using a 29-gauge needle. For each injection, a new syringe and needle were used. After retracting the eyelids, the bulbar conjunctiva was gently grasped and tented up with forceps. The needle was kept tangential to the globe and was inserted through the conjunctiva. A bleb of fluid was immediately apparent as the injection was performed. Dose formulations were administered in both eyes at a volume of 100 µl/eye and a target dose level of 1 mg/eye. The control groups (groups 1 and 5) were administered with 100 µl/eye of formulation vehicle only. Immediately following treatment, the eyes were examined (indirect ophthalmoscopy and slit-lamp biomicroscopy), and any abnormalities caused by the dosing procedure were documented.

Sample Collection

Blood samples (2–3 ml) were collected from the auricular artery of all animals in groups 2, 3, and 4 (three animals per time point per group) at 0.5, 1, 6, 12, 24, 48, and 96 h postdose. Blood (2–3 ml) was collected from the auricular artery of all animals in groups 1 and 5 (six animals in total) shortly after administration of the formulation vehicle. Immediately following blood collection, animals were euthanized by intravenous injection of Euthanyl® (MTC Pharmaceuticals, Cambridge, Ontario, Canada). The eyes were removed and dissected to collect the aqueous fluid and vitreous fluid (each sample pooled for two eyes).

Sample Processing

Following collection, blood was separated into two aliquots, one (500–750 µl) to provide a whole-blood sample and the remainder for the preparation of plasma. Both aliquots were transferred to Vacutainer™ (BD Diagnostics, Franklin Lakes, NJ, USA) tubes containing potassium ethylenediaminetetraacetic acid and kept on wet ice. The larger portion was centrifuged (4°C at 2700 rpm for approximately 10 min) within 1 h of collection. The plasma samples were then separated into two, approximately equal, portions and were placed on dry ice until storage at approximately −80°C. The whole-blood sample was also transferred to storage at approximately −80°C.

Aqueous Fluid and Plasma Sample Analysis

All samples were kept frozen at approximately −80°C until analysis, at which time samples were allowed to thaw to room temperature. Plasma and aqueous fluid were analyzed for the concentration and content of aptamers using a hybridization-based dual-capture assay.

Hybridization-Based Dual-Capture Assay for Aptamer Quantitation

The analytical method used to measure the concentration of intact aptamer in plasma and aqueous humor samples was a Good Laboratory Practice-validated hybridization-based dual-capture pseudo-ELISA assay based on the method of Healy *et al.* (12). In this assay, a biotinylated capture probe (5′ ACTCTGTAATAACCCC-[spacer18]-biotin) was pre-immobilized in the wells of a 96-well Reacti-Bind™ Neutravidin-coated polystyrene plate (Pierce Chemical, Rockford, IL, USA) at a binding solution concentration of ~10 nM (100 µl/well; ~1 pmol/well) during a 2 h incubation, covered, at room temperature with shaking at approximately 800 rpm. Excess unbound probe was removed by washing five times with wash buffer (1× PBS, 0.05% Tween-20, 200 µl/well), followed by blotting on absorbent paper to remove excess liquid. SuperBlock™ blocking buffer (in PBS, 200 µl/well; Pierce Chemical) was added to all wells (either for a 2 h incubation, covered, at room temperature while shaking at approximately 800 rpm, or for an overnight incubation at approximately 4°C). The SuperBlock™ blocking buffer was then removed, and plates were washed five times with wash buffer followed by blotting on absorbent paper. In separate tubes, calibration standards, quality control (QC) samples, and analytical samples were diluted (typically 1:5–1:1000-fold) in dilution buffer (4× saline sodium citrate, 0.05% Tween-20), then 180 µl of the diluted solutions was preannealed in a buffer containing 300 µl of the FAM-labeled (5′-6-carboxyfluorescein phosphoramidite modifier; Glen Research, Sterling, VA, USA) detection probe (5′ FAM-[spacer18]-GGGTACAGCTATACAG, at 200 nM) and 120 µl of dilution buffer at 90°C for 15 min, then cooled down in an ice water bath for at least 5 min and centrifuged at 15,000 rpm for approximately 5 min at 4°C. A 120 µl aliquot of the preannealed standards, controls, and analytical samples were then pipetted into the Reacti-Bind™ Neutravidin-coated plates containing the immobilized biotin capture probe, followed by an incubation for approximately 2.5 h, covered, at approximately 45°C in a 100% humidity environment. After the hybridization reaction was completed, plates were washed five times with wash buffer followed by blotting on absorbent paper. Next, a detection antibody [antifluorescein, rabbit IgG, conjugated to horseradish peroxidase (HRP)] was added to plates (100 µl/well of a 0.1 µg/ml solution in 1× PBS; Molecular Probes, Eugene, OR, USA) for approximately 1 h, covered, at room temperature. The plates were then washed five times with wash buffer followed by blotting on absorbent paper. Signal generation was accomplished by adding 100 µl/well of a solution containing a fluorogenic HRP substrate (QuantaBlu™, Pierce Chemical) and incubated, covered, and protected from light for 30 min at approximately 30°C. The signal generation reaction was then stopped by the addition of 100 µl/well of Quantablue® stopping solution (Pierce Chemical), and the fluorescence intensity from each well was read using a SpectraMax Gemini spectrofluorimeter (Molecular Devices, Sunnyvale, CA, USA; excitation wavelength 325 nm/emission wavelength 420 nm, 10 reads/well). The fluorescence signal generated in each well was proportional to the concentration of aptamer present. Data reduction from the microplate reader is performed using SOFTmax PRO, version 4.0. A four-parameter logistic (4PL) model is used to fit the sigmoid calibration curve. A semilogarithmic sigmoid calibration curve is obtained by plotting the fluorescence response against concentration. The mathematical equation and the

four parameters (A, B, C, and D) characterizing the curve by the 4PL model are as follows:

$$Y = \frac{A - D}{1 + (X/C)^B} + D$$

where Y is the response variable, X is the concentration, A is the response (predicted) at zero concentration, B is the slope factor (slope of the plot), C is the concentration midpoint between A and D, and D is the response at infinite concentration.

Concentrations of full-length aptamer in the test samples were determined by computer interpolation from the plot of the calibration standard curve. The lower limit of quantitation (LLOQ) for this assay was approximately 1 ng/ml (oligo mass) or 0.1 nM.

Pharmacokinetic Data Analysis

Noncompartmental pharmacokinetic parameters (t_{max}, C_{max}, AUC, k_{el}, $t_{1/2}$) of test article in aqueous fluid and plasma were estimated using standard noncompartmental analysis (NCA) using standard software (SAS version 8.1). The C_{max} was obtained by data inspection. The AUC was calculated by application of the trapezoidal rule (16), and k_{el} was obtained by linear regression analysis of selected time points in the terminal phase of the concentration *vs.* time curves. The apparent terminal half-life ($t_{1/2}$) was calculated as follows: $t_{1/2} = \ln(2)/k_{el}$.

RESULTS

Determination of Aptamer Affinity for TGFβ2 Protein

The nucleotide sequence and predicted secondary structure of anti-TGFβ2 aptamer ARC81 (32-mer) is shown in Fig. 1 and in Materials and Methods. Except for one minor alteration (removal of an A/U base pair in the terminal stem), ARC81 shares the same base sequence with the transcribed aptamer ARC77, originally identified on the basis of high-affinity binding to human TGFβ2 using SELEX (14). However, ARC81 contains several modifications for

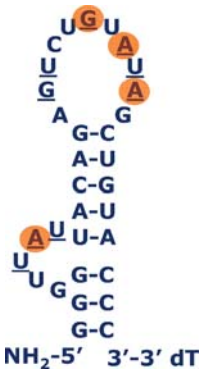

Fig. 1. Predicted secondary structure of anti-TGFβ2 aptamer, ARC81.

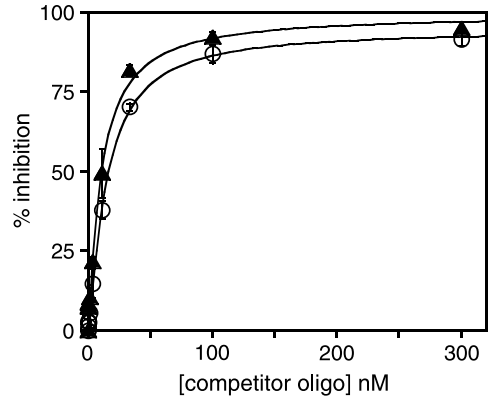

Fig. 2. Binding affinity of anti-TGFβ2 aptamers for purified TGFβ2 protein.

protection against nuclease digestion, consisting of 2′-methoxy substitutions at various positions within the backbone and a 3′-3′-linked thymidine added to the 3′-terminus.

The affinity (K_D) of ARC77 for TGFβ2 was estimated to be 1.4 ± 0.2 nM, as determined by nitrocellulose filtration using radiolabeled aptamer. However, we found that methylation of the aptamer backbone resulted in substantial nonspecific sticking to the nitrocellulose membrane, which interfered with the assay. Therefore, in the present work, we determined the binding affinity of ARC81 to purified human and rabbit TGFβ2 (human and rabbit isoforms of TGFβ2 are identical in amino acid sequence) using a competition assay, in which cold ARC81 (or ARC77) was added as an inhibitor of the interaction between TGFβ2 and radiolabeled ARC77. Dissociation constants of approximately 4 and 5 nM were determined for the binding of cold ARC77 and ARC81 to TGFβ2, respectively (Fig. 2). Because TGFβ2 is a homodimer, each TGFβ2 complex has the potential to interact with as many as two aptamer molecules, simultaneously, when aptamer is in excess. Although there is no direct evidence demonstrating multiple aptamer binding, the ~2-fold discrepancy in dissociation constants measured by the two assay methods would be consistent with this possibility.

Pharmacologic Activity of TGFβ2 Aptamers

Cross-reactivity of ARC81 with human and rabbit TGFβ2, combined with the fact that rabbit models are used widely for preclinical testing of ocular anti-scarring agents, prompted us to: (1) evaluate bioactivity of ARC81 *in vitro* in rabbit aqueous humor, an endogenous source of TGFβ2 protein; and (2) examine ocular and plasma pharmacokinetic properties in rabbit of ARC81 and its PEGylated derivatives. Inclusion of an amine-modifying group at the 5′-terminus of ARC81 (Fig. 1) facilitated chemical conjugation with polyethylene glycol polymers to generate aptamers ARC117 (20 kDa PEG) and ARC119 (40 kDa PEG). Presence of 5′-terminal PEG groups did not significantly alter *in vitro* affinity of aptamers for purified TGFβ2 in competition binding assays (data not shown).

TGFβ2 had been shown previously to inhibit proliferation *in vitro* of MLEC (17). Thus, a MLEC proliferation bioassay was established to test activity of aptamers against

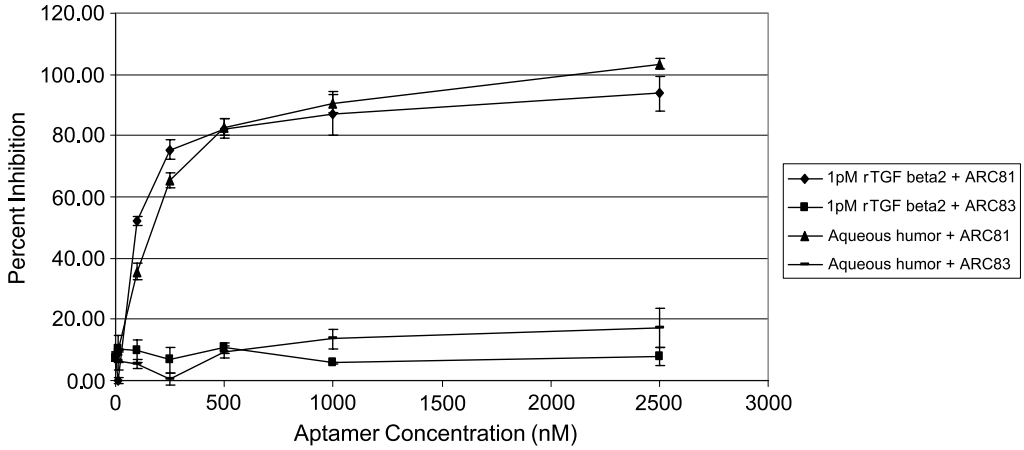

Fig. 3. Anti-TGFβ2 aptamer-mediated neutralization of TGFβ2 activity.

purified TGFβ2 and TGFβ2 present in rabbit aqueous humor. Figure 3 shows that the ARC81 aptamer inhibited the antiproliferative effects of purified recombinant TGFβ2. An anti-TGFβ2 antibody (R&D Systems, AF-302-NA), tested as a control, also reversed the effect of purified TGFβ2 in the MLEC assay (data not shown). These data indicate that ARC81 is able to reverse the biological activity of purified TGFβ2 as measured using cell proliferation with an IC_{50} of approximately 100 nM. Because eventual utility of an anti-TGFβ2 therapeutic aptamer could require activity in aqueous humor, we also tested the ability of aptamers to inhibit native TGFβ2 in a rabbit ocular fluid matrix. As shown in Fig. 3, ARC81 reversed aqueous-humor-mediated inhibition of MLEC proliferation. Anti-TGFβ2 antibody, used as a control, also reversed the effect of low concentrations of aqueous humor on cell proliferation (data not shown). Figure 3 shows further that ARC81 rescued rabbit aqueous-humor-mediated inhibition of MLEC proliferation in a dose-dependent manner. ARC81 blocked endogenously derived TGFβ2 in rabbit aqueous humor with an IC_{50} of approximately 200 nM and an IC_{90} of approximately 1 μM. Taken together, these data indicate that the ARC81 aptamer is able to reverse the biological activity of TGFβ2 in aqueous humor.

Pharmacokinetic Profiles of ARC81 and PEGylated Aptamer Conjugates

We next assessed whether anti-TGFβ2 aptamers administered via a single subconjunctival injection would reach the ocular aqueous humor in sufficient concentration, and with appropriate pharmacokinetic half-life, to provide a sustained therapeutic benefit upon daily or weekly administration in the rabbit subconjunctival scarring model. Subconjunctival injection has been demonstrated to be an effective means of delivering anti-scarring agents directly to the surgical site (19). A pharmacokinetic study was performed to determine the pharmacokinetics of ARC81 (no PEG) and PEG-conjugated derivatives ARC117 (20 kDa PEG) and ARC119 (40 kDa PEG) anti-TGFβ2 aptamers following administration to rabbits via subconjunctival injection. These aptamers were formulated at a concentration of 10 mg/ml (oligo mass), administered bilaterally at a dose of 1 mg/eye, and plasma and ocular fluid samples collected at 0, 0.5, 1, 2, 6, 12, 24, 48, and 96 h post-administration as described in Materials and Methods. Figures 4–8 show the aqueous humor or plasma concentration of each aptamer (in ng/ml) over an interval of 50 h following subconjunctival administration. Table I tabulates estimated pharmacokinetic parameters at a

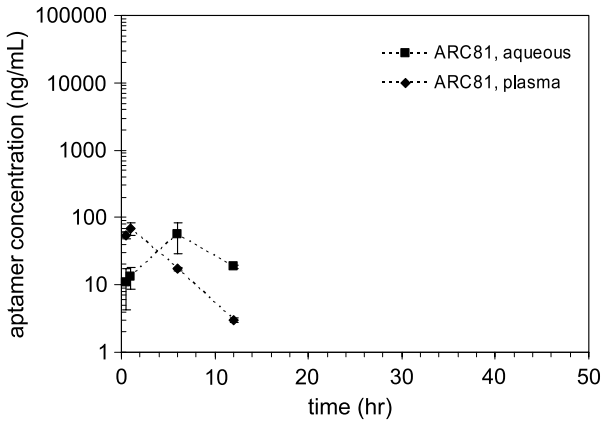

Fig. 4. Pharmacokinetic profiles of anti-TGFβ2 aptamer ARC81 in plasma and aqueous humor.

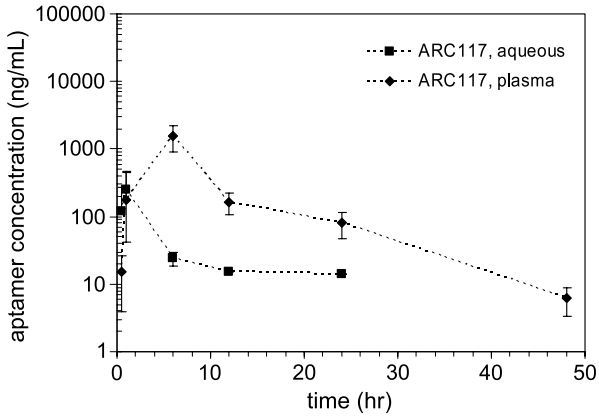

Fig. 5. Pharmacokinetic profiles of PEGylated anti-TGFβ2 aptamer ARC117 (20 kDa) in plasma and aqueous humor.

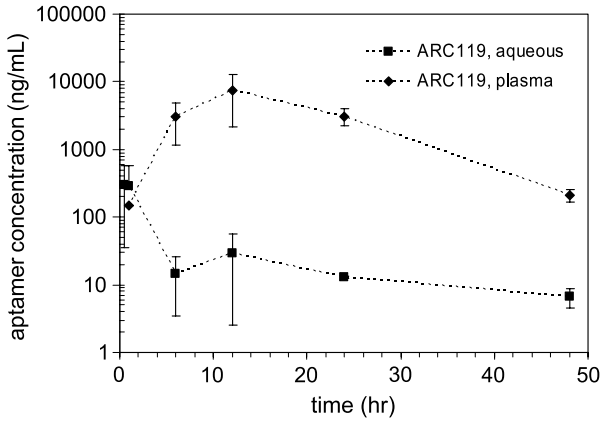

Fig. 6. Pharmacokinetic profiles of PEGylated anti-TGFβ2 aptamer ARC119 (40 kDa) in plasma and aqueous humor.

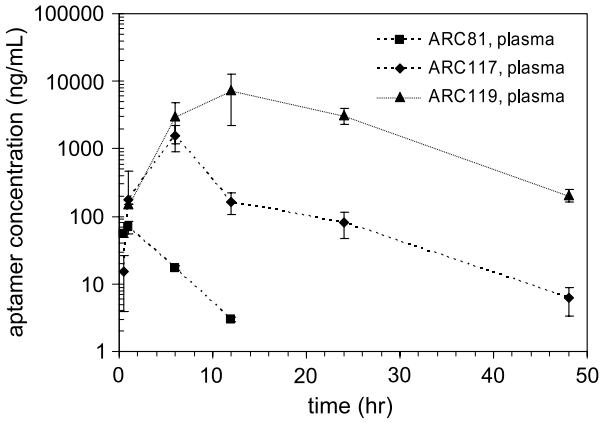

Fig. 8. Comparison of aptamer pharmacokinetics in plasma.

dose of 1 mg/eye bilaterally (i.e., 2.0 mg/animal) as determined by NCA.

ARC81 (no PEG), ARC117 (20 kDa PEG), and ARC119 (40 kDa PEG) were all detected in aqueous humor after subconjunctival administration (Figs. 4–6). Unconjugated aptamer (ARC81) entered systemic circulation rapidly (by 0.5 h) and peaked by approximately 1 h post-dose (Fig. 4). Thereafter, concentrations declined rapidly to less than the limit of quantitation (LLOQ), indicating rapid clearance of unconjugated aptamer from plasma. The maximum concentration of unconjugated aptamer in aqueous humor showed a delayed t_{max}, possibly because of recirculation of aptamer from the blood stream (Table I). Both PEG-conjugated aptamers ARC117 (20 kDa PEG) and ARC119 (40 kDa PEG) showed similar plasma elimination half-lives ($t_{1/2} \simeq 7$ h) and achieved higher maximal concentrations (C_{max}) in aqueous humor and plasma relative to unconjugated aptamer (Figs. 5 and 6, Table I). The timing (t_{max}) with which maximal concentrations of PEGylated aptamers were achieved in plasma was delayed for both ARC117 (20 kDa PEG; t_{max} = 6 h) and ARC119 (40 kDa PEG; t_{max} = 12 h) compared to unPEGylated aptamer (ARC81; t_{max} = 1 h). The delayed t_{max} values seen for PEG-conjugated aptamers in plasma imply existence of a significant depot effect in vicinity of injection site (Fig. 8 and Table I). Clearance from both plasma and aqueous compartments was generally slower for the PEGylated molecules (ARC117 and ARC119) than for unconjugated aptamer (ARC81) (Figs. 7 and 8).

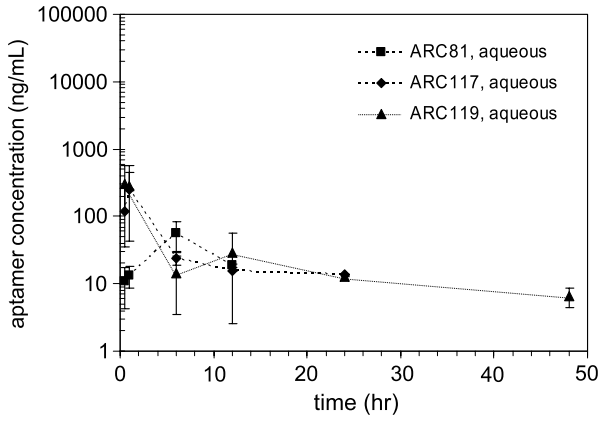

Fig. 7. Comparison of aptamer pharmacokinetics in aqueous humor.

DISCUSSION

In general, concentrations and exposure of the rabbits to aptamers were greater for ARC119 (40 kDa PEG) and ARC117 (20 kDa PEG) than for ARC81 (unconjugated) in both plasma and aqueous fluid (i.e., ARC119 > ARC117 > ARC81). For all aptamers, plasma levels were higher than corresponding levels measured in aqueous fluid. ARC81 (no PEG) was cleared more rapidly from the eye than aptamer conjugates ARC117 (20 kDa PEG) and ARC119 (40 kDa PEG), which showed prolonged residence in the aqueous compartment. Both 20- and 40-kDa aptamer conjugates reached maximal concentrations (C_{max}) in aqueous humor of 246–304 ng/ml (oligo mass; ~23–30 nM, respectively) and remained at or above 10 ng/ml (oligo mass; ~1 nM) for as long as 12 h. There seemed to be a correlation in plasma between t_{max} and the size of the molecules, with the PEGylated aptamers (ARC117 and ARC119) passing into systemic circulation much more slowly than the non-PEGylated aptamer (ARC81). Thus, the effects of PEGylation seem to include retention of the aptamer in the subconjunctival space, thereby facilitating transport to the aqueous compartment, and hindrance of subsequent filtration from the aqueous to the plasma compartments.

Previously, in surgical models of conjunctival scarring in rabbits, inhibition of TGFβ2 at the surgical site (i.e., in the subconjunctival space and aqueous compartment), by either a monoclonal antibody or by an antisense oligonucleotides, has been shown to prevent ocular scar formation such as that seen in trabeculectomy, a surgical procedure that is a common treatment for primary open angle glaucoma. Anti-TGFβ2 aptamer cross-reacts with both rabbit and human TGFβ2 isoforms and is active in the ocular fluid environment of aqueous humor. The capacity of the aptamers, regardless of PEGylation, to elicit mechanistic blockade of TGFβ2-mediated cellular proliferation in a cell-based assay utilizing TGFβ2 from rabbit aqueous humor suggests that this species-specific model of conjunctival scarring may provide an appropriate experimental system to evaluate the biological efficacy of PEGylated forms of anti-

Table I. Pharmacokinetic Parameters of Aptamers in Plasma and Aqueous Humor

		Plasma			Aqueous		
Parameter	Unit	ARC81	ARC117	ARC119	ARC81	ARC117	ARC119
PEG	kDa	None	20	40	None	20	40
t_{max}	h	1	6	12	6	1	0.5
t_{last}	h	12	48	48	12	6	48
C_{max}	ng/ml	69.2	1576	7468	55.8	246	304
$AUC_{0-tlast}$	ng·h/ml	321	12,177	143,739	405	797	1584
AUC_{0-inf}	ng·h/ml	331	12,243	145,795	nc	nc	1829
k_{el}	h^{-1}	0.287	0.094	0.101	nc	nc	0.027
$t_{1/2}$	h	2.42	7.4	6.84	nc	nc	25.8

All aptamer concentrations are calculated using total mass = oligo mass + PEG mass.
nc = not calculated (insufficient data points available to define the elimination phase of the concentration *vs.* time profile); PEG = polyethylene glycol.

TGFβ2 aptamers. Furthermore, from our initial pharmacokinetic evaluation of PEGylated anti-TGFβ2 aptamers ARC117 (20 kDa PEG) and ARC119 (40 kDa PEG), administered via subconjunctival injection to the rabbit eye, we conclude that these agents reach a sufficient exposure level (1000-fold greater than the measured concentration of TGFβ2 in the aqueous humor of glaucomatous eyes) and exhibit prolonged residence times in subconjunctival space and aqueous compartment to suggest that aptamer-derived therapeutic agents may prove to be effective drugs for the prevention of postsurgical ocular scar formation. In addition, reduced volumes of distribution (V_d) and delayed timing (t_{max}) at which maximal concentrations of PEGylated anti-TGFβ2 aptamers appeared in plasma implies a depot effect in the vicinity of the injection site.

In conclusion, we have generated an aptamer inhibitor of rabbit and human forms of TGFβ2 protein that is active in the ocular fluid environment of aqueous humor. The capacity of the ARC81-series aptamers to elicit mechanistic blockade of TGFβ2-mediated cellular proliferation in a cell-based assay utilizing TGFβ2 from rabbit aqueous humor suggests that this species-specific model of conjunctival scarring may provide an appropriate experimental system to evaluate the biological efficacy of PEGylated forms of anti-TGFβ2 aptamers. Furthermore, from our initial pharmacokinetic evaluation of PEGylated anti-TGFβ2 aptamers ARC117 (20 kDa PEG) and ARC119 (40 kDa PEG), administered via subconjunctival injection to the rabbit eye, we conclude that these agents reach a sufficient local exposure level and exhibit significantly prolonged residence times to suggest that aptamer-derived therapeutic agents could prove to be effective drugs for the prevention of postsurgical ocular scar formation.

ACKNOWLEDGEMENTS

The authors thank Dr. Sandra Dennis and Dr. John Nash at CTBR-BioResearch Inc. (Montreal, Quebec, Canada) for support of this study and Dr. Judy Healy (Archemix Corp., Cambridge, MA, USA) for help with preparation of the manuscript.

REFERENCES

1. C. Verges, J. Cazal, and C. Lavin. Surgical strategies in patients with cataract and glaucoma. *Curr Opin Ophthalmol* **16**:44–52 (2005).
2. R. Bindlish, G. P. Condon, J. D. Schlosser, J. D'Antonio, K. B. Lauer, and R. Lehrer. Efficacy and safety of mitomycin-C in primary trabeculectomy: five-year follow-up. *Ophthalmology* **109**:discussion 1341–1342 (2002).
3. D. A. Belyea, J. A. Dan, R. L. Stamper, M. F. Lieberman, and W. H. Spencer. Late onset of sequential multifocal bleb leaks after glaucoma filtration surgery with 5-fluorouracil and mitomycin C. *Am J Ophthalmol* **124**:40–45 (1997).
4. T. H. Kupin, M. S. Juzych, D. H. Shin, A. K. Khatana, and M. M. Olivier. Adjunctive mitomycin C in primary trabeculectomy in phakic eyes. *Am J Ophthalmol* **119**:30–39 (1995).
5. W. L. Membrey, D. P. Poinoosawmy, C. Bunce, F. W. Fitzke, and R. A. Hitchings. Comparison of visual field progression in patients with normal pressure glaucoma between eyes with and without visual field loss that threatens fixation. *Br J Ophthalmol* **84**:1154–1158 (2000).
6. Y. Ochiai and H. Ochiai. Higher concentration of transforming growth factor-beta in aqueous humor of glaucomatous eyes and diabetic eyes. *Jpn J Ophthalmol* **46**:249–253 (2002).
7. M. F. Cordeiro, M. B. Reichel, J. A. Gay, F. D'Esposita, R. A. Alexander, and P. T. Khaw. Transforming growth factor-beta1, -beta2, and -beta3 *in vivo*: effects on normal and mitomycin C-modulated conjunctival scarring. *Investig Ophthalmol Vis Sci* **40**:1975–1982 (1999).
8. M. F. Cordeiro, J. A. Gay, and P. T. Khaw. Human anti-transforming growth factor-beta2 antibody: a new glaucoma anti-scarring agent. *Investig Ophthalmol Vis Sci* **40**:2225–2234 (1999).
9. M. F. Cordeiro, A. Mead, R. R. Ali, R. A. Alexander, S. Murray, C. Chen, C. York-Defalco, N. M. Dean, G. S. Schultz, and P. T. Khaw. Novel antisense oligonucleotides targeting TGF-beta inhibit *in vivo* scarring and improve surgical outcome. *Gene Ther* **10**:59–71 (2003).
10. C. Tuerk and L. Gold. Systematic evolution of ligands by exponential enrichment: RNA ligands to bacteriophage T4 DNA polymerase. *Science* **249**:505–510 (1990).
11. W. A. Pieken, D. B. Olsen, F. Benseler, H. Aurup, and F. Eckstein. Kinetic characterization of ribonuclease-resistant 2′-modified hammerhead ribozymes. *Science* **253**:314–317 (1991).
12. J. M. Healy, S. D. Lewis, M. Kurz, R. M. Boomer, K. T. Thompson, C. Wilson, and T. G. McCauley. Pharmacokinetics and biodistribution of novel aptamer compositions. *Pharm Res* **21**:2234–2246 (2004).
13. S. R. Watson, Y. F. Chang, D. O'Connell, L. Weigand, S. Ringquist, and D. H. Parma. Anti-L-selectin aptamers: binding

characteristics, pharmacokinetic parameters, and activity against an intravascular target *in vivo*. *Antisense Nucleic Acid Drug Dev* **10**:63–75 (2000).
14. N. Pagratis, M. Lochrie, and L. Gold. High affinity TGFβ nucleic acid ligands and inhibitors, Gilead Sciences, Inc., USA, United States Patent No. 63,466,111, 2002.
15. P.E. Burmeister, S. D. Lewis, R. F. Silva, J. R. Preiss, L. R. Horwitz, P. S. Pendergrast, T. G. McCauley, J. C. Kurz, D. M. Epstein, C. Wilson, and A. D. Keefe. Direct *in vitro* selection of a 2′-*O*-methyl aptamer to VEGF. *Chem Biol* **12**:25–33 (2005).
16. M. Gibaldi and D. Perrier. *Pharmacokinetics*, Marcel Dekker Inc., New York, 1982.
17. J. C. Jennings, S. Mohan, T. A. Linkhart, R. Widstrom, and D. J. Baylink. Comparison of the biological actions of TGF beta-1 and TGF beta-2: differential activity in endothelial cells. *J Cell Physiol* **137**:167–172 (1988).
18. S. W. Cousins, M. M. McCabe, D. Danielpour, and J. W. Streilein. Identification of transforming growth factor-beta as an immunosuppressive factor in aqueous humor. *Investig Ophthalmol Vis Sci* **32**:2201–2211 (1991).
19. A. L. Mead, T. T. Wong, M. F. Cordeiro, I. K. Anderson, and P. T. Khaw. Evaluation of anti-TGF-beta2 antibody as a new postoperative anti-scarring agent in glaucoma surgery. *Investig Ophthalmol Vis Sci* **44**:3394–3401 (2003).